



Low-voltage organic n-channel thin-film transistors based on a core-cyanated perylene tetracarboxylic diimide derivative

Ute Zschieschang, Konstantin Amsharov, R. Thomas Weitz, Martin Jansen, Hagen Klauk*

Max Planck Institute for Solid State Research, Heisenbergstr. 1, 70569 Stuttgart, Germany

ARTICLE INFO

Article history:

Received 24 July 2008

Received in revised form 17 July 2009

Accepted 22 July 2009

Available online 20 August 2009

Keywords:

Organic thin-film transistors

Organic complementary circuits

ABSTRACT

Using the small-molecule organic semiconductor bis(1*H*,1*H*-perfluorobutyl)-dicyano-perylene tetracarboxylic diimide, C₃F₇CH₂-PTCDI-(CN)₂, and a low-temperature-processed, high-capacitance gate dielectric based on a phosphonic acid self-assembled monolayer, we have manufactured n-channel thin-film transistors on glass substrates. The transistors operate with low voltages (2 V) and have an electron mobility of 0.04 cm²/Vs and an on/off ratio of 10⁵. By combining C₃F₇CH₂-PTCDI-(CN)₂ n-channel transistors with pentacene p-channel transistors, we have also manufactured low-voltage, low-power organic complementary inverters with good static and dynamic performance.

© 2009 Elsevier B.V. All rights reserved.

1. Introduction

Organic thin-film transistors (TFTs) and organic integrated circuits that can be operated with low voltages (about 3 V or less) are of interest for a variety of electronic applications, such as low-power active-matrix displays for portable devices. Low-voltage organic TFTs can be realized by implementing a gate dielectric with a capacitance close to 10⁻⁶ F/cm². Ideally, these gate dielectrics are based on materials that can be processed at temperatures below about 150 °C, so that the TFTs and circuits can be manufactured on flexible polymeric substrates. Materials that have been utilized for the fabrication of low-temperature, high-capacitance gate dielectrics for organic TFTs include sputtered, evaporated or anodically grown thin metal oxides [1–8], organic self-assembled monolayers [9–18], organic self-assembled multilayers [19–22], and thin insulating polymers [23–26]. Most of the work on low-voltage organic TFTs so far has focused on p-channel transistors. A few reports on low-voltage organic n-channel TFTs exist, although they either utilized organic semiconductors that rapidly degrade in air and thus need to be characterized in an inert atmosphere [4,17] or suffer from small charge carrier field-effect mobilities (0.02 cm²/Vs or less) [8,12,18,19,23,24]. Here we report on air-stable low-voltage organic n-channel transistors on glass substrates utilizing a core-cyanated perylene diimide derivative as the semiconductor and a thin, high-capacitance, low-temperature-processed gate dielectric based on a phosphonic acid self-assembled monolayer. These TFTs can be operated with voltages of 3 V and have an electron mobility of 0.04 cm²/Vs in air.

The synthesis of the small-molecule organic semiconductor, bis(1*H*,1*H*-perfluorobutyl)-dicyano-perylene tetracarboxylic diimide, C₃F₇CH₂-PTCDI-(CN)₂, was first reported by Michael Ahrens and coworkers in 2003 [27]. Organic n-channel TFTs based on this semiconductor were first reported by Brooks Jones and coworkers in 2004 [28] and 2007 [29]. Using a heavily doped silicon wafer as the substrate and gate electrode and a 300 nm thick thermally grown SiO₂ layer as the gate dielectric, Jones et al. manufactured air-stable C₃F₇CH₂-PTCDI-(CN)₂ TFTs with electron field-effect mobilities of 0.64 cm²/Vs [28] and 0.24 cm²/Vs [29], depending on the gate dielectric functionalization. These transistors required operating voltages of 100 V. For a C₃F₇CH₂-PTCDI-(CN)₂ TFT with a similar device structure and a slightly thinner gate dielectric (100 nm), Weitz et al. recently reported a mobility of 0.1 cm²/Vs, also measured in air, but using operating voltages of 15 V [30]. The air stability of C₃F₇CH₂-PTCDI-(CN)₂ transistors is a consequence of the electronegative substituents and the relatively large electron affinity of the semiconductor (4.5 eV; [28,29]). The large field-effect mobility is related to the crystal packing [28–30]. To synthesize the organic semiconductor C₃F₇CH₂-PTCDI-(CN)₂ we followed the procedure reported by Jones et al. [28,30].

2. Experimental

The TFTs were manufactured on a glass substrate using the inverted staggered (bottom-gate, top-contact) device structure. Gate electrodes were prepared by evaporating aluminum with a thickness of 20 nm through a shadow mask. The aluminum gates were briefly exposed to an oxygen plasma to create a hydroxyl-terminated aluminum oxide film and then immersed in a 2-propanol solution of commercially available

* Corresponding author.

E-mail address: H.Klauk@fkf.mpg.de (H. Klauk).

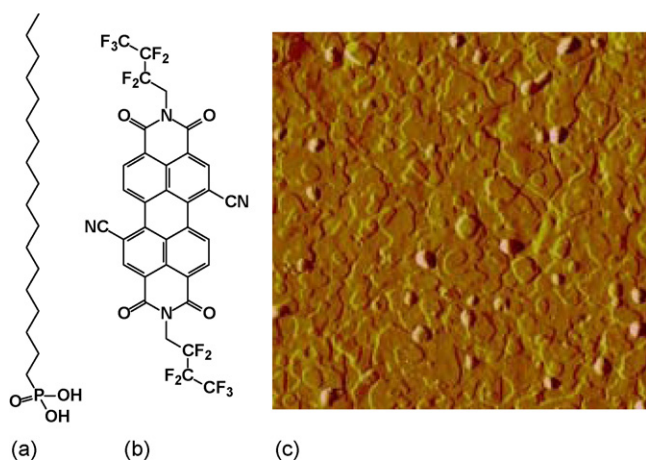


Fig. 1. (a) Chemical structure of *n*-octadecylphosphonic acid, utilized for the self-assembled monolayer gate dielectric. (b) Chemical structure of the organic semiconductor $C_3F_7CH_2$ -PTCDI-(CN) $_2$. (c) Atomic force microscopy (AFM) image of a 30 nm thick, vacuum-deposited film of $C_3F_7CH_2$ -PTCDI-(CN) $_2$.

n-octadecylphosphonic acid (chemical structure shown in Fig. 1a) to allow an organic monolayer to self-assemble on the oxidized aluminum surface. After about 16 h, the substrate was removed from solution, rinsed with 2-propanol, dried in a stream of nitrogen, and briefly baked on a hotplate at a temperature of 60 °C. Thus, the gate dielectric consists of a 3.6 nm thick aluminum oxide film and a 2.1 nm thick self-assembled monolayer. A 30 nm thick film of $C_3F_7CH_2$ -PTCDI-(CN) $_2$ (chemical structure shown in Fig. 1b) was then deposited by sublimation in vacuum, again through a shadow mask. During the deposition of the organic semiconductor, the substrate temperature was maintained at 120 °C. Finally, 30 nm thick gold source/drain contacts were deposited by evaporation

through another shadow mask. All electrical measurements were carried out in ambient air.

3. Results and discussion

Fig. 1c shows an atomic force microscopy (AFM) image of a 30 nm thick film of $C_3F_7CH_2$ -PTCDI-(CN) $_2$ deposited by sublimation in a vacuum evaporator while the substrate was held at a temperature of 120 °C. At this substrate temperature, $C_3F_7CH_2$ -PTCDI-(CN) $_2$ forms polycrystalline films with full surface coverage and relatively large grains [30].

A photograph of a completed $C_3F_7CH_2$ -PTCDI-(CN) $_2$ transistor with a channel length of 50 μm and a channel width of 200 μm is shown in Fig. 2a. The electrical characteristics of this TFT are shown in Fig. 2b and c. Owing to the large gate dielectric capacitance (0.7 $\mu\text{F}/\text{cm}^2$) the transistor can be operated with voltages of 3 V. The TFT has a subthreshold swing of 160 mV/decade, an on/off ratio of 10^5 , and a threshold voltage of -0.8 V. In Fig. 2d the electron mobility (μ) is plotted as a function of the applied gate-source voltage (V_{GS}), calculated using the standard formalism for field-effect transistors operating in the saturation regime: $\mu = 2 \cdot L / (W \cdot C) \cdot (\partial \sqrt{I_D} / \partial V_{GS})^2$, where L is the channel length (50 μm), W is the channel width (200 μm), C is the dielectric capacitance (0.7 $\mu\text{F}/\text{cm}^2$), and I_D is the drain current [12]. As can be seen, for gate-source voltages above about -0.2 V the electron mobility is about 0.04 cm^2/Vs . To our knowledge, this is the largest mobility reported for an air-stable low-voltage organic n-channel TFT.

To realize a low-voltage organic complementary inverter we have combined a $C_3F_7CH_2$ -PTCDI-(CN) $_2$ n-channel TFT and a pentacene p-channel TFT in a shadow-mask-patterned layout on a glass substrate. Both TFTs have a channel length of 50 μm . The circuit schematic is shown in Fig. 3a. Fig. 3b shows an oscilloscope snapshot of a dynamic test of the inverter where a square-wave input

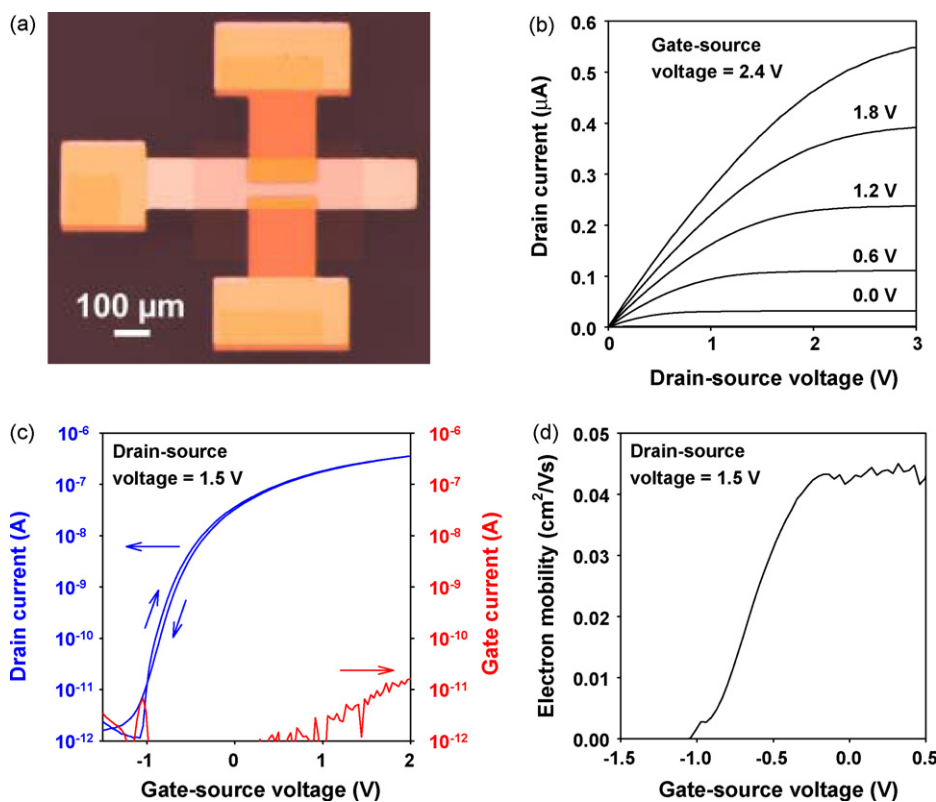


Fig. 2. (a) Photograph of a $C_3F_7CH_2$ -PTCDI-(CN) $_2$ transistor with a channel length of 50 μm and a channel width of 200 μm . (b) Output characteristics of the transistor. (c) Transfer characteristics of the same transistor, all measured in ambient air. (d) Electron mobility as a function of gate-source voltage.

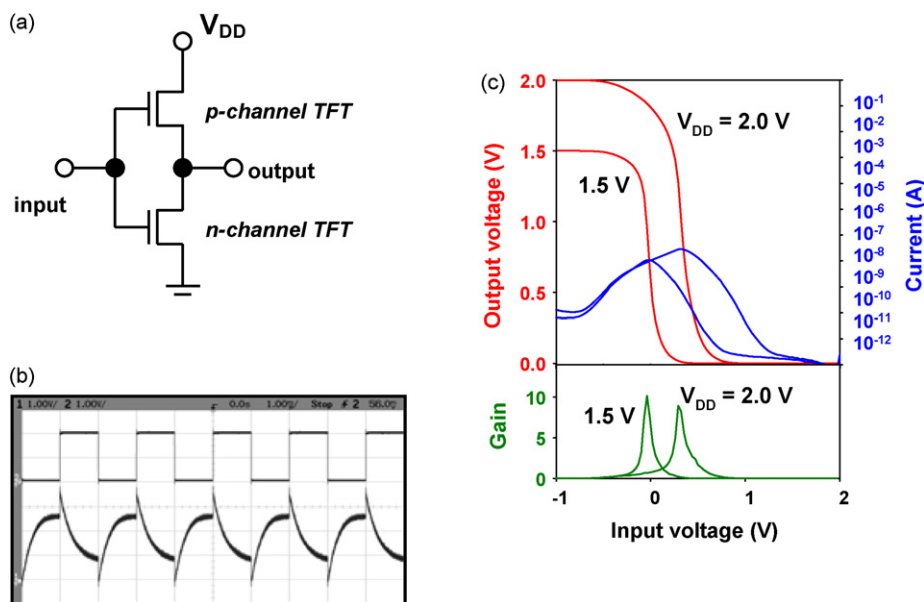


Fig. 3. (a) Circuit schematic of a complementary inverter. (b) Dynamic response of a complementary inverter based on a $C_3F_7CH_2$ -PTCDI-(CN)₂ n-channel and a pentacene p-channel transistor to a square-wave input signal with a frequency of 500 Hz (top: input signal; bottom: output signal). (c) Static transfer characteristics of the inverter for supply voltages of 1.5 and 2 V.

signal with an amplitude of 2 V and a frequency of 500 Hz is applied to the input of the inverter. The output signal shows the correct response of the inverter. Fig. 3c shows the static transfer characteristics of the inverter for supply voltages of 1.5 and 2 V. The inverter shows sharp switching and rail-to-rail output swings for both supply voltages, with a small-signal gain of about 10. Compared with inverters based on a single carrier type [13,14], complementary inverters consume less static power, since one of the two transistors is always in the non-conducting off-state, except during switching. The static current of the inverter in Fig. 3 is less than 100 pA, so the static power dissipation is less than 200 W per logic gate.

4. Conclusions

In summary, we have realized air-stable low-voltage organic n-channel thin-film transistors with an electron mobility of $0.04 \text{ cm}^2/\text{Vs}$ and an on/off ratio of 10^5 , using the small-molecule organic semiconductor bis(1*H*,1*H*-perfluorobutyl)-dicyanoperylene tetracarboxylic diimide, $C_3F_7CH_2$ -PTCDI-(CN)₂, and a thin gate dielectric based on a phosphonic acid self-assembled monolayer. In combination with a low-voltage pentacene p-channel TFT we have also manufactured low-voltage organic complementary inverters with good static and dynamic performance and small static power dissipation.

Acknowledgements

The authors thank Benjamin Stuhlhofer at the Max Planck Institute for Solid State Research for expert technical assistance and Richard Rook at CADILAC Laser for providing high-quality shadow masks.

References

[1] C.D. Dimitrakopoulos, S. Purushothaman, J. Kymissis, A. Callegari, J.M. Shaw, *Science* 283 (1999) 822.
 [2] L.A. Majewski, R. Schroeder, M. Voigt, M. Grell, *J. Phys. D: Appl. Phys.* 37 (2004) 3367.

[3] C.S. Kim, S.J. Jo, S.W. Lee, W.J. Kim, H.K. Baik, S.J. Lee, D.K. Hwang, S. Im, *Appl. Phys. Lett.* 88 (2006) 243515.
 [4] M. Kitamura, Y. Arakawa, *Appl. Phys. Lett.* 91 (2007) 53505.
 [5] J. Tardy, M. Erouel, A.L. Deman, A. Gagnaire, V. Teodorescu, M.G. Blanchin, B. Canut, A. Barau, M. Zaharescu, *Microelectronics Reliability* 47 (2007) 372.
 [6] M. Zirkl, A. Haase, A. Fian, H. Schön, C. Sommer, G. Jakopic, G. Leising, B. Stadlober, I. Graz, N. Gaar, R. Schwödiauer, S. Bauer-Gogonea, S. Bauer, *Adv. Mater.* 19 (2007) 2241.
 [7] M.F. Chang, P.T. Lee, S.P. McAlister, A. Chin, *IEEE Electr. Dev. Lett.* 29 (2008) 215.
 [8] A. Fian, A. Haase, B. Stadlober, G. Jakopic, N.B. Matsko, W. Grogger, G. Leising, *Anal. Bioanal. Chem.* 390 (2008) 1455.
 [9] J. Collet, O. Tharaud, A. Chapoton, D. Vuillaume, *Appl. Phys. Lett.* 76 (2000) 1941.
 [10] M. Halik, H. Klauk, U. Zschieschang, G. Schmid, C. Dehm, M. Schütz, S. Maisch, F. Effenberger, M. Brunnbauer, F. Stellacci, *Nature* 431 (2004) 963.
 [11] Y.D. Park, D.H. Kim, Y. Jang, M. Hwang, J.A. Lim, K. Cho, *Appl. Phys. Lett.* 87 (2005) 243509.
 [12] H. Klauk, U. Zschieschang, J. Pflaum, M. Halik, *Nature* 445 (2007) 745.
 [13] H. Klauk, U. Zschieschang, M. Halik, *J. Appl. Phys.* 102 (2007) 074514.
 [14] H. Klauk, U. Zschieschang, R.T. Weitz, H. Meng, F. Sun, G. Nunes, D.E. Keys, C.R. Fincher, Z. Xiang, *Adv. Mater.* 19 (2007) 3882.
 [15] H. Ma, O. Acton, G. Ting, J.W. Ka, H.L. Yip, N. Tucker, R. Schofield, A.K.Y. Jen, *Appl. Phys. Lett.* 92 (2008) 113303.
 [16] T. Sekitani, Y. Noguchi, U. Zschieschang, H. Klauk, T. Someya, *Proc. Natl. Acad. Sci.* 105 (2008) 4976.
 [17] P.H. Wöbkenberg, J. Ball, F.B. Kooistra, J.C. Hummelen, D.M. deLeeuw, D.D.C. Bradley, T.D. Anthopoulos, *Appl. Phys. Lett.* 93 (2008) 013303.
 [18] U. Zschieschang, M. Halik, H. Klauk, *Langmuir* 24 (2008) 1665.
 [19] M.H. Yoon, A. Facchetti, T.J. Marks, *Proc. Natl. Acad. Sci.* 102 (2005) 4678.
 [20] B.H. Lee, M.K. Ryu, S.Y. Choi, K.H. Lee, S. Im, M.M. Sung, *J. Am. Chem. Soc.* 129 (2007) 16034.
 [21] K.H. Lee, J.M. Choi, S. Im, B.H. Lee, K.K. Im, M.M. Sung, S. Lee, *Appl. Phys. Lett.* 91 (2007) 123502.
 [22] S.A. DiBenedetto, D. Frattarelli, M.A. Ratner, A. Facchetti, T.J. Marks, *J. Am. Chem. Soc.* 130 (2008) 7528.
 [23] M.H. Yoon, H. Yan, A. Facchetti, T.J. Marks, *J. Am. Chem. Soc.* 127 (2005) 10388.
 [24] A. Facchetti, M.H. Yoon, T.J. Marks, *J. Am. Chem. Soc.* 128 (2006) 4928.
 [25] S.H. Kim, S.Y. Yang, K. Shin, H. Jeon, J.W. Lee, K.P. Hong, C.E. Park, *Appl. Phys. Lett.* 89 (2006) 83516.
 [26] S.Y. Yang, S.H. Kim, K. Shin, H. Jeon, C.E. Park, *Appl. Phys. Lett.* 88 (2006) 173507.
 [27] M.J. Ahrens, M.J. Fuller, M.R. Wasielewski, *Chem. Mater.* 15 (2003) 2684.
 [28] B.A. Jones, M.J. Ahrens, M.H. Yoon, A. Facchetti, T.J. Marks, M.R. Wasielewski, *Angew. Chem. Int. Ed.* 43 (2004) 6363.
 [29] B.A. Jones, A. Facchetti, M.R. Wasielewski, T.J. Marks, *J. Am. Chem. Soc.* 129 (2007) 15259.
 [30] R.T. Weitz, K. Amsharov, U. Zschieschang, E. Barrena Villas, D.K. Goswami, M. Burghard, H. Dosch, M. Jansen, K. Kern, H. Klauk, *J. Am. Chem. Soc.* 130 (2008) 4637.